

The Sensitivity of Infall Molecular Line Profiles to the Ambient Radiation Field

M.P. Redman^{1,2}, J.M.C. Rawlings¹, J.A. Yates¹ and D.A. Williams¹

¹Department of Physics and Astronomy, University College London, Gower Street, London WC1E 6BT, UK

¹School of Cosmic Physics, Dublin Institute for Advanced Studies, 5 Merrion Square, Dublin 2, Ireland

arXiv:astro-ph/0404198v1 8 Apr 2004

Received **insert**; in original form **insert**

ABSTRACT

In cold molecular clouds submillimetre emission lines are excited by the ambient radiation field. The pumping is dominated by the cosmic microwave background (CMB). It is usual in molecular line radiative transfer modelling to simply assume that this is the only incident radiation field. In this paper, a molecular line transport code and a dust radiative transfer code are used to explore the effects of the inclusion of a full interstellar radiation field (ISRF) on a simple test molecular cloud. It is found that in many galactic situations, the shape and strength of the line profiles that result are robust to variations in the ISRF and thus that in most cases, it is safe to adopt the CMB radiation field for the molecular line transport calculations. However, we show that in two examples, the inclusion of a plausible radiation field can have a significant effect on the the line profiles. Firstly, in the vicinity of an embedded massive star, there will be an enhanced far infrared component to the radiation field. Secondly, for molecular clouds at large redshift, the CMB temperature increases and this of course also alters the radiation field. In both of these cases, the line profiles are weakened significantly compared to a cloud exposed to a standard radiation field. Therefore this effect should be accounted for when investigating prestellar cores in massive star forming regions and when searching for molecular clouds at high redshift.

Key words: line:profiles - radiative transfer - stars:formation - ISM:clouds - ISM:kinematics and dynamics - ISM:molecules

1 INTRODUCTION

Molecular line profiles from prestellar and protostellar objects can potentially yield dynamical information about the collapse process that leads to the formation of stars. In the last decade or so, the common practice has been to obtain line profiles from an infall candidate and then to use a radiative transfer code, together with a dynamical model to interpret the data. Inferences are then made about the validity of one or other of the competing star formation models. However, it is becoming clear that the interpretation of these line profiles can be fraught with difficulty. Rawlings & Yates (2001) used a self-consistent chemical and dynamical model of collapsing star-forming cores to explore the effects of abundance variations. They showed that the line profiles are very sensitive to the assumed values of the free parameters in the chemical models.

Ward-Thompson & Buckley (2001) have presented a sensitivity analysis of the line profiles to various free parameters, in the context of modelling the Class 0 sources, NGC1333-IRAS2 and Serpens SMM4. The STENHOLM ra-

ditive transfer code (see, e.g. Heaton et al. 1993) was used, adopting analytical fits to the Shu (1977) collapse model for the velocity and density profiles, and an optically thin thermal balance model for the dust temperature. The following free parameters were investigated: the impact parameter, or beam offset from the central position, the beam size (or assumed source distance), the infall velocity, the fractional abundances of the tracer species (assumed not to vary with position), the turbulent velocity and the systemic rotational velocity. One of the most important (general) findings was that the qualitative shape of the line profiles - in particular the velocity separation between the red- and blue-shifted peaks in the self-reversed line profiles is highly sensitive to the turbulent velocity. This results from the broadening of the absorption profiles of the foreground envelope, whilst the total integrated flux increases with the turbulent velocity dispersion as the effective optical depth of the emitting gas is reduced.

In this paper, the results of numerical experiments to investigate the sensitivity of molecular line profiles to the radiation field incident on a realistic test globule are reported.

Firstly, the effects on molecular line profiles of changing this field from the CMB to a more realistic ISRF is investigated. Secondly, the ISRF is modified to simulate the radiation field in the vicinity of embedded massive stars. Finally the ISRF is modified by increasing the CMB temperature, to simulate the radiation field in which molecular clouds at high-redshift will be found. Our study lacks the more self-consistent approach of the combined hydrodynamical/chemical/radiative transfer models of Rawlings and Yates (2001), but serves to show the sensitivities and hence to highlight the diagnostic strengths (and weaknesses) of line profile analyses.

The discussion is limited to two well known molecular tracers used to diagnose collapsing cores: HCO^+ ($J=3 \rightarrow 2$) and ^{13}CO ($J=2 \rightarrow 1, 3 \rightarrow 2$). This allows direct comparison with other work; previous studies (eg. Rawlings and Yates, 2001) have shown that the HCO^+ transition is particularly likely to be strongly self-reversed and asymmetric, whilst the effects on the CO lines has implications for high-redshift molecular observations. The discussion is also limited to zero beam offset positions so as to allow a simple comparison of the effects discussed in this paper.

2 RADIATIVE TRANSFER MODELLING OF SUBMILLIMETRE LINE EMISSION

The radiative transfer code used in this work is SMMOL, an approximate Λ -iterative code that solves multi-level non-LTE radiative transfer problems (see Rawlings & Yates 2001 for full details). The results generated by this code can be viewed with some confidence because a series of recent benchmarking exercises have compared several such codes, including for example RATRAN, an accelerated Monte-Carlo code described by Hogerheijde & van der Tak (2000). Both SMMOL and RATRAN, despite the very different numerical methods used, are able to yield the same results when applied to test cases very similar to the model runs described here. The benchmarking has been described by van Zadelhoff et al. (2002).

For our numerical studies, a test globule was constructed using the class 0 source B335, which is one of the best observed (and modelled) protostellar infall candidates (e.g. Zhou et al. 1993; Choi et al. 1995; Wilner et al. 2000). The physical parameters of the test globule (following Rawlings & Yates 2001) are based upon the models of B335 of Zhou et al. (1993) and Choi et al. (1995). At each of fifty points in a radial grid (similar to that of Choi et al. 1995) the radius, density, fractional abundance, gas temperature, dust temperature, radial velocity and microturbulent velocity are specified. The density and velocity profiles [$n(r)$ and $v(r)$] are taken from the Shu (1977) inside-out collapse model, with the physical parameters as specified in Table 1. B335 is being used because there is a well developed model for it, but it is not claimed that B335 itself is being subjected to any of the effects explored in this paper.

Modifying the radiation field incident on the globule will affect the dust temperature. To account for this, the dust temperature in the globule is calculated for each radiation field using the dust radiative transfer code described in Efstathiou & Rowan-Robinson (1994). For the case of a standard ISRF at $z=0$, it was verified that the radial profile of the dust temperature is comparable to that deduced from

dust continuum observations of B335 (Zhou et al., 1990). As in Rawlings and Yates (2001), we assume that the dust and gas are thermally well coupled. Although this assumption is probably not valid in the low density ($n < 10^5 \text{ cm}^{-3}$) outer envelope, we again note that it holds in the denser line-forming core regions. In fact, the dust/gas temperature changes turn out to only have a second order effect on the line profiles compared with changing the radiation field. The collapse model is not well-justified, and more reliable evaluations of the temperature profile are now available (Shirley et al. 2000) but this approach provides a useful and well-known benchmark against which to test the effects discussed in this paper.

Most of the transitions that we consider in this study are very optically thick, so that the line profiles are relatively insensitive to the absolute values of the fractional abundances (X_i). This result is in marked difference to the findings of Ward-Thompson and Buckley (2000) who found strong qualitative and quantitative differences when X_i was varied between $10^{-9} - 10^{-8}$. We suspect that this is a result of the inability of the STENHOLM code to deal with extreme optical depths. However, as emphasised in Rawlings and Yates (2000), radial *variations* in the abundances can have profound effects on the line profiles. We do not want to confuse the interpretation of our results with chemical issues, so we simply adopt a two-phase chemical scheme, with separate abundances within and exterior to the infall radius (r_{inf}); Choi et al. (1995) used a single constant abundance in their work. The abundances used in our model - which are spatial averages taken from fig. 1 of Rawlings and Yates (2000), are also given in Table 1.

3 INCLUSION OF A FULL INTERSTELLAR RADIATION FIELD

Most molecular line transport codes adopt the CMB as the incident radiation field van Zadelhoff et al. (2002). While this is the dominant source of radiation at the wavelengths of the molecular transitions under consideration here, a proper treatment should include the full interstellar radiation field. van Dishoeck (1994) has reviewed how such a radiation field is constructed. It contains three dominant components: starlight (mainly from B stars), dust-enshrouded massive stars, and the CMB. It is these latter two components that are modified in this work and discussed below. Firstly though, the effect of replacing the CMB with a realistic ISRF was investigated. In this work, the radiation field constructed by Evans et al. (2001) was employed. This is a combination of the radiation field introduced by Black (1994) with that of Draine (1978). The dust radiative transfer code was used to firstly calculate the gas/dust temperature before the line profiles were generated by the molecular line transport code.

The inclusion of the Black-Draine ISRF had almost no discernible effect on the line profile shapes for both species. This is because the CMB component of the radiation field vastly dominates the line formation at these wavelengths. Therefore, in most galactic environments, it is safe to simply adopt the CMB as the only significant incident radiation field. The ISRF of Mathis et al. (1983) is a plausible alternative radiation field but using this produced little discernible

Cloud radius	0.15 pc
Collapse age (t_{coll})	1.36×10^5 years
Infall radius (r_{inf})	0.03 pc
Distance to source	250 pc
Telescope diameter	15 m
Beam efficiency	0.6
$X(\text{HCO}^+)$	5×10^{-9} ($r < r_{\text{inf}}$) 5×10^{-10} ($r > r_{\text{inf}}$)
$X(^{13}\text{CO})$	1×10^{-7} ($r < r_{\text{inf}}$) 2×10^{-7} ($r > r_{\text{inf}}$)

Table 1. Parameters used in the dynamical and radiative transfer model.

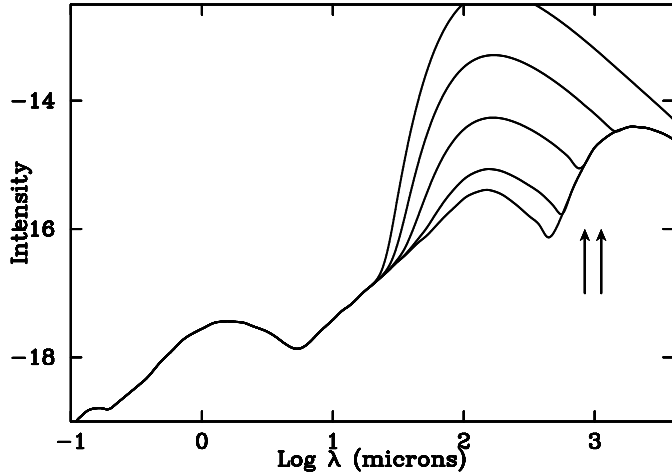


Figure 1. Black and Draine radiation field with an additional component due to a nearby embedded massive star. This is represented by a 30 K blackbody, scaled by factors of 10^{-4} , 10^{-3} , 10^{-2} , 10^{-1} to represent variations in the fractional sky coverage of the embedded object. The two arrows mark the wavelengths of the HCO^+ $J = 3 \rightarrow 2$ and $J = 4 \rightarrow 3$ lines. The intensity scale is logarithmic with units of $\text{erg s}^{-1} \text{cm}^{-2} \text{Hz}^{-1} \text{sr}^{-1}$

difference in the line profiles. However, the dust continuum strength will be affected by the UV and IR photons and is sensitive to the exact form of the radiation field used.

4 VARYING THE INCIDENT RADIATION FIELD ON A GALACTIC GLOBULE

The embedded massive star component in the ISRF is particularly important since the few forming massive stars are typically accompanied by huge numbers of low mass star forming objects. The radiation peak from an embedded massive star typically occurs at around $100 \mu\text{m}$ and can be approximated as a blackbody of temperature ~ 30 K (e.g. Chini et al. 1987). In diffuse clouds the contribution of the massive star radiation field is several orders of magnitude less than the CMB at the wavelengths of molecular line tracer transitions, simply because of the small covering fraction on the sky of these regions. However, in the vicinity of a hot core or embedded UCH II region the fraction of the sky occupied by the cloud may be large enough that the radiation field at mm wavelengths is enhanced.

Figure 1 is a plot of the Black-Draine ISRF to which has been added a 30 K grey body to represent the increased flux due to an embedded massive star component. The ratio of the grey body to black body flux is varied between 10^{-2}

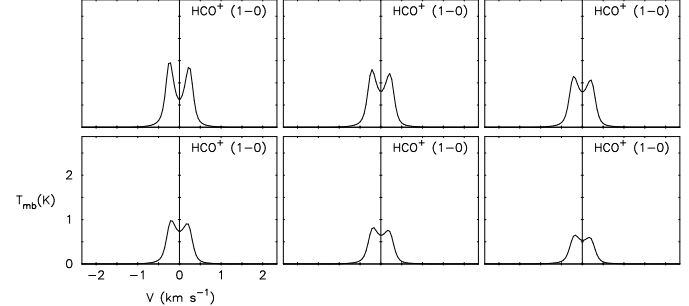


Figure 2. Model HCO^+ $1 \rightarrow 0$ line profiles for a Black-Draine radiation field with a diluted 30 K blackbody. From top left to right the dilution factor has the following values: 0.01, 0.1, 0.15, 0.2, 0.25, 0.3

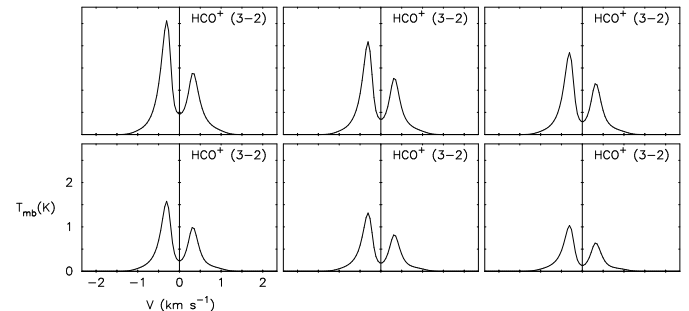


Figure 3. Model HCO^+ $3 \rightarrow 2$ line profiles for a Black-Draine radiation field with a diluted 30 K blackbody. From top left to right the dilution factor has the following values: 0.01, 0.1, 0.15, 0.2, 0.25, 0.3

and 3×10^{-1} . Of course, using an isotropic grey body flux is a crude simplification of the real situation of an adjacent localised radiation source, a point returned to in Section 6. The two arrows mark the wavelengths of the HCO^+ $J = 3 \rightarrow 2$ and $J = 4 \rightarrow 3$ lines. It can be seen that once the flux ratio exceeds around 10^{-2} , the mm continuum flux at the wavelengths of the lines is altered significantly.

Figures 2-5 are ^{13}CO and HCO^+ line profiles from the test globule for the different radiation fields. Inspection of the profiles indicates that the line strengths are significantly reduced when the globule is exposed to increasing ambient radiation. The effect is slightly more pronounced in the lowest transitions of both of the species. Similar results obtain for calculations of the line profiles of CS, which for brevity are not presented here. In other words, if a cloud is close enough to an embedded massive star that over around one percent of the sky is occupied then it will not be valid to

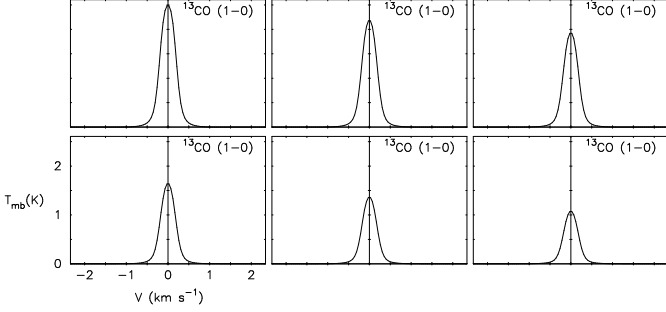


Figure 4. Model ^{13}CO $3 \rightarrow 2$ line profiles for a Black-Draine radiation field with a diluted 30 K blackbody. From top left to right the dilution factor has the following values: 0.01, 0.1, 0.15, 0.2, 0.25, 0.3

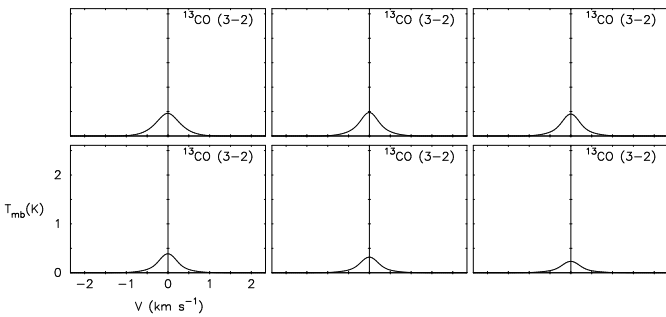


Figure 5. Model ^{13}CO $1 \rightarrow 0$ line profiles for a Black-Draine radiation field with a diluted 30 K blackbody. From top left to right the dilution factor has the following values: 0.01, 0.1, 0.15, 0.2, 0.25, 0.3

simply adopt a CMB radiation field: the diluted embedded massive star component must be added to it first. For example, the sizes of the envelopes surrounding massive stars are of order $\sim 10^{18}$ cm and so any starless cloud within a few parsecs will be exposed to a significant flux of mm photons from the tail of the blackbody from the embedded star. Thus any future studies of individuals from the thousands of low mass stars that form in the vicinity of high mass stars should take this effect into account.

5 VARYING THE INCIDENT RADIATION FIELD ON A HIGH REDSHIFT GLOBULE

Star formation appears to have peaked at a redshift of around $z = 1$ and appears to have been occurring as early as $z = 6.4$ (Walter et al. 2003, Bertoldi et al. 2003 and see e.g. Illingworth 1999 for a review of the subject). The first appearance and evolution of molecular gas in galaxies over this time is also very uncertain. Norman & Spaans (1997) have discussed the formation of molecules at high redshift. While at present the observational difficulties of studying high redshift molecular clouds are severe, it is nonetheless interesting to consider the effects of the warmer CMB radiation field at earlier epochs and its effect on any molecular clouds present then. To investigate this, the Black and Draine radiation field above was modified by varying the CMB temperature component with redshift such that

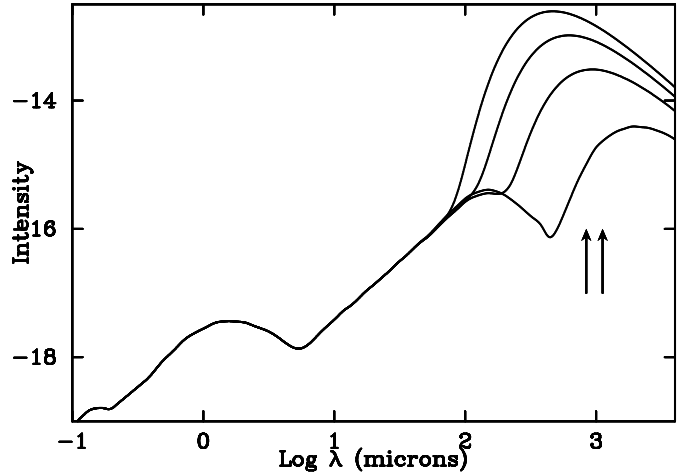


Figure 6. Black and Draine radiation field at high redshift. The CMB component increases with redshift. Displayed are the radiation fields for $z=0$ (lowermost curve), 1, 2, and 3 (uppermost curve). The two arrows mark the wavelengths of the HCO^+ $J = 3 \rightarrow 2$ and $J = 4 \rightarrow 3$ lines. The intensity scale is logarithmic with units of $\text{erg s}^{-1} \text{cm}^{-2} \text{Hz}^{-1} \text{sr}^{-1}$.

$$\frac{T_z}{T_{\text{cmb}}} = 1 + z, \quad (1)$$

where T_{cmb} is the current CMB temperature of 2.728 K. Values of z up to 3 were considered. The shapes of the radiation field produced by these values of z are displayed in Figure 6. As before, the modification of the internal temperature structure by dust heating produces only second order changes to the line profile shape. The most significant changes are caused by the change in CMB temperature, as discussed below.

With the model specified as above, we considered variations in the incident FIR and mm-wave radiation field on the cloud as the only free parameter. This is initially provided by the Cosmic Microwave Background (CMB) radiation, characterised by a black-body of temperature 2.728K. The radiation is assumed to be isotropic and illuminates the exterior of the cloud. We alter the value of the FIR and mm-wave radiation field by specifying different radiation temperatures (T_{rad}) corresponding to redshifts of 0, 1, 2, and 3 according to equation 1.

Varying the incident radiation field in this way has an even more dramatic effect than the changes described in Section 4 - the line profiles of each of the three tracers become progressively weaker as the temperature rises, until at the highest temperatures considered in this study ($\simeq 11$ K) they almost vanish. Higher temperature runs (not presented here) were also carried out and show that the profiles even move into absorption with increasing temperature.

Figs 7-10 show the continuum-subtracted line profiles generated for the HCO^+ ($J=3 \rightarrow 2$) and ($J=1 \rightarrow 0$) and the ^{13}CO ($J=3 \rightarrow 2$) and ($J=1 \rightarrow 0$) transitions respectively, for different values of the external radiation temperature. The gradual suppression of the emission line profile with increasing temperature is immediately clear. The numerical experiment shows how a bright FIR/mm-wave radiation field can greatly diminish ^{13}CO emission.

Clearly the gas in a globule of thermal temperature of around 10K embedded in a medium with a thermal temper-

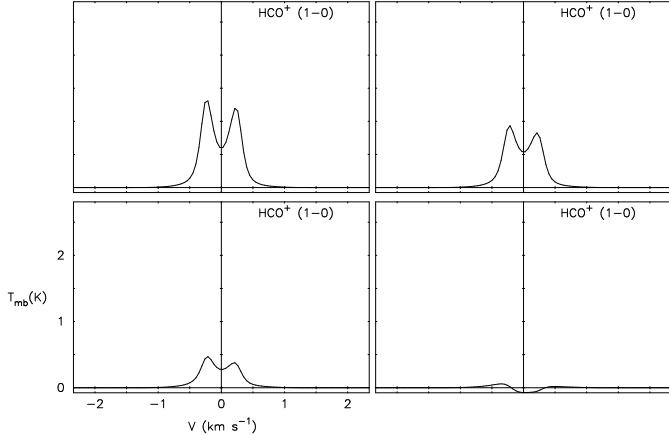


Figure 7. Model HCO^+ 1 → 0 line profiles for a Black-Draine radiation field modified such that the CMB temperature is that appropriate for high redshift. From top left to right the redshifts are: 0, 1, 2, 3

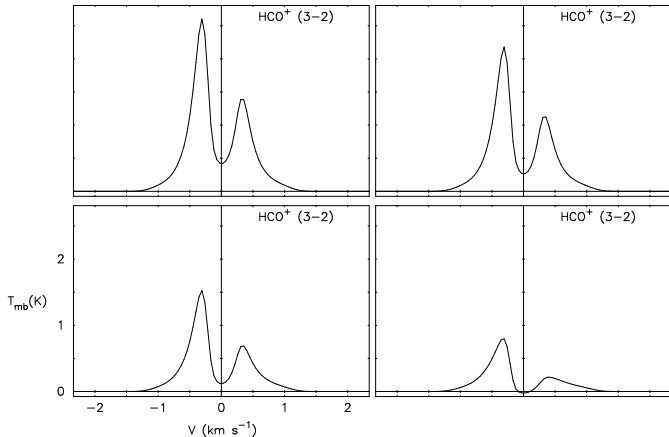


Figure 8. Model HCO^+ 3 → 2 line profiles for a Black-Draine radiation field modified such that the CMB temperature is that appropriate for high redshift. From top left to right the redshifts are: 0, 1, 2, 3

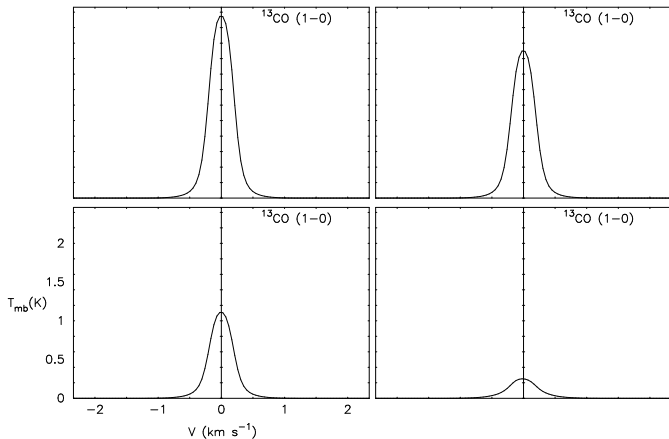


Figure 9. Model ^{13}CO 1 → 0 line profiles for a Black-Draine radiation field modified such that the CMB temperature is that appropriate for high redshift. From top left to right the redshifts are: 0, 1, 2, 3

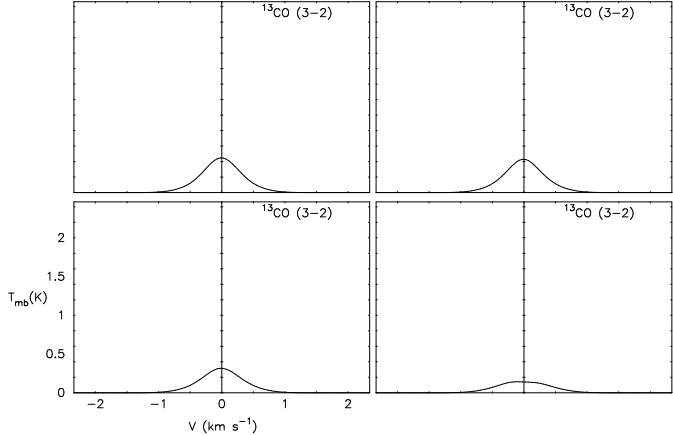


Figure 10. Model ^{13}CO 3 → 2 line profiles for a Black-Draine radiation field modified such that the CMB temperature is that appropriate for high redshift. From top left to right the redshifts are: 0, 1, 2, 3

ature of say, 20K, will absorb the background radiation via molecular lines. What has been overlooked before however is that even a low temperature background will affect the line profiles. Since the separation of energy levels in many of these species is of the order of a few Kelvin, extra external photons will have the effect of increased pumping of the energy levels of the molecules. This results in increased absorption in the lower J levels and emission from high J levels.

6 IMPLICATIONS AND OBSERVATIONAL TESTS

The results presented here suggest that in most cases interpretations of fits to observational line profiles will be satisfactory since the background radiation field does approximate the CMB. However, for an isolated Bok globule in the vicinity of some newly formed massive stars, for example, characterising the incident as well as the local radiation field will be an indispensable first step in modelling the line profiles. Our adoption of a grey body isotropic addition to the radiation field is clearly a simplification. It seems likely that the use of non-isotropic background radiation field could yield line profile shapes that vary in strength across a source.

Several straight forward observational tests could be carried out to verify the effects described here. Firstly, a sample of protostellar cores of similar evolutionary status but situated in quite different ambient medium conditions could be observed. The prediction is that the objects in the hotter environments that lead to significant dust heating and re-radiation at millimetre and sub-millimetre wavelengths will have weaker molecular emission in the low-lying transitions as compared to their more embedded counterparts. However, the strength of the higher level transitions (such as $\text{HCO}^+ J=4 \rightarrow 3$) will be marginally less affected. Observations of several lines could therefore be used to diagnose the environment of star-forming regions. A second test would be to identify a source that is non-uniformly illuminated by the background radiation e.g. an object lying close to the edge of

a massive star forming region. The morphological distribution, as traced by the sort of low-lying transitions described above will be biased by the effects described in this paper and should result in the spatial peak of the molecular distribution being offset (towards the cooler side of the object) from the density (continuum) peak. It is possible that the effects discussed in this paper may be partly responsible for some of the offsets between the spatial peaks in the various molecular tracers and the continuum that have been observed towards certain star-forming regions. It should be cautioned however that it will be difficult to separate these effects from those of variations in chemical abundances and kinetic temperature.

One example of a star-forming location in which the external radiation is likely to differ significantly from the CMB is the Eagle nebula. White et al. (1999) detected sub-mm emission peaks towards the heads of the famous columns. They found that the dust temperature ranges from 250-320K in the hot outer layers to 10-20K deep in the columns. Clearly, the evaporating gaseous globules (Hester et al. 1996) on the outside of the columns will be subject to much harsher environment than to clumps in the sub-mm column and to isolated B335-like cores. Similarly, Beuther et al. (2000) find a temperature gradient from 70K to below 20K across the Cepheus B molecular cloud which, like the Eagle, has a massive star heating one side of the cloud.

Most interestingly, White et al. (1999) note with concern that in the sub-mm peaks in the columns of the Eagle nebula, the (1-0) transitions in CO and its isotopes are all 2-3 times weaker than would be expected based on the strengths of higher transitions. This has implications for the common practice of using CO and ^{13}CO to measure cloud masses. White et al suggest that freeze-out of CO may have occurred in the coldest parts of the core. Our results may also naturally explain these anomalies - the lowest transition is being weakened by changes to the level populations due to the radiation field from the nearby massive stars.

The higher CMB temperature at high redshift has a clear effect on the line profile shapes and the suppression of the line strengths could potentially lead to extra difficulties in the detection of molecular clouds at redshifts $z > 1$.

7 CONCLUSIONS AND FUTURE WORK

It has been argued that the intensity and shape of sub-millimetre molecular line profiles as modelled by radiative transfer codes of prestellar and protostellar cores are sensitive to the long-wavelength ambient radiation field illuminating the exterior of the cloud. Some caution is therefore suggested in the modelling of observational results - the ambient environment must somehow be constrained before fitting profiles and making conclusions about the dynamics and chemical composition of the system.

It should be noted that the effect described here is not unknown to workers in computational radiative transfer (it was discussed at the benchmarking exercise that led to the paper by Van Zadelhoff et al 2002), in preparation). However, this is the first time that the astrophysical consequences of this effect have been explored in any detail. In future papers on star-formation, we will - following the pre-

liminary study of Ward-Thompson & Buckley 2001) - address the issue of how the velocity structure in general, and the microturbulent velocity in particular, affects the line profiles. It is important to realise that it is essential to characterise correctly the microphysics of potential infall sources. This will eventually allow more robust inferences to be made from line profile data than is currently possible.

ACKNOWLEDGEMENTS

MPR and DAW were supported by PPARC and the Leverhulme Trust respectively while this work was carried out. Some of the calculations described here were carried out on the Miracle Supercomputer, at the HiPerSPACE computing Centre, UCL, which is funded by the UK Particle Physics and Astronomy Research Council.

REFERENCES

Bertoldi F., Cox P., Neri R., Carilli C. L., Walter F., Omont A., Beelen A., Henkel C., Fan X., Strauss M. A., Menten K. M., 2003, *ApJ*, 409, L47
 Beuther H., Kramer C., Deiss B., Stutzki J., 2000, *A&A*, 362, 1109
 Black J. H., 1994, in ASP Conf. Ser. 58: The First Symposium on the Infrared Cirrus and Diffuse Interstellar Clouds Energy Budgets of Diffuse Clouds. p. 355
 Chini R., Krügel E., Wargau W., 1987, *A&A*, 181, 378
 Choi M., Evans II N. J., Gregeren E. M., Wang Y., 1995, *ApJ*, 448, 742
 Draine B. T., 1978, *ApJS*, 36, 595
 Efstathiou A., Rowan-Robinson M., 1994, *MNRAS*, 266, 212
 Evans N. J., Rawlings J. M. C., Shirley Y. L., Mundy L. G., 2001, *ApJ*, 557, 193
 Heaton P. M., Little L. T., Yamashita T., Davies S. R., Cunningham C. T., Monteiro T. S., 1993, *A&A*, 278, 238
 Hester J. J., Scowen P. A., Sankrit R., and E. A. Ajhar T. R. L., Baum W. A., Code A., Currie D. G., and S. P. Ewald G. E. D., Faber S. M., Grillmair C. J., Groth E. J., Holtzman J. A., Hunter D. A., Kristian J., Light R. M., Lynds C. R., Monet D. G., O'Neil E. J., Shaya E. J., Seidelman K. P., Westphal J. A., 1996, *AJ*, 111, 2349
 Hogerheijde M. R., van der Tak F. F. S., 2000, *A&A*, 362, 697
 Illingworth G., 1999, *apss*, 269, 165
 Mathis J. S., Mezger P. G., Panagia N., 1983, *A&A*, 128, 212
 Norman C. A., Spaans M., 1997, *ApJ*, 480, 145
 Rawlings J. M. C., Yates J. A., 2001, *MNRAS*, 326, 1423
 Shirley Y. L., Evans N. J., Rawlings J. M. C., Gregeren E., 2000, *ApJS*, 131, 249
 Shu F. H., 1977, *ApJ*, 214, 488
 van Dishoeck E. F., 1994, in ASP Conf. Ser. 58: The First Symposium on the Infrared Cirrus and Diffuse Interstellar Clouds Photochemistry and the Interstellar Radiation Field. p. 319
 van Zadelhoff G.-J., Dullemond C. P., van der Tak F. F. S., Yates J. A., Doty S. D., Ossenkopf V., Hogerheijde M. R.,

Juvela M., Wiesemeyer H., Schöier F. L., 2002, A&A, 395, 373

Walter F., Bertoldi F., Carilli C., Cox P., Lo K. Y., Neri R., Fan X., Omont A., Strauss M. A., Menten K. M., 2003, Nature, 424, 406

Ward-Thompson D., Buckley H. D., 2001, MNRAS, 327, 955

White G. J., Nelson R. P., Holland W. S., et al 1999, A&A, 342, 233

Wilner D. J., Myers P. C., Mardones D., Tafalla M., 2000, ApJ, 544, L69

Zhou S., Evans II N. J., Kömpe C., Walmsley C. M., 1993, ApJ, 404, 232